

First-principles studies of electrophilic molecules on the carbon nanotubes

Sohee Park, Ki-jeong Kong, Hye-Mi So, Gyoung-Ho Buh, Jeong-O Lee, and Hyunju Chang*

Fusion Biotechnology Research Center, Advanced Materials Division
Korea Research Institute of Chemical Technology
P. O. Box 107, Daejeon, 305-600, Korea, hjchang@kriict.re.kr

ABSTRACT

Various approaches have been made to separate semiconducting carbon nanotubes (CNTs) from metallic ones including chemical treatments. Recently we have demonstrated that some electrophilic molecules, such as 2,4,6-triphenylpyrylium tetrafluoroborate (2,4,6-TPPT) and 1,3-benzodithiolylium tetrafluoroborate (1,3-BDYT), preferentially interact with metallic CNTs. In this study, we present systematic theoretical studies on the interactions between the CNTs and these electrophilic molecules, using density functional theory. It was found that 2,4,6-TPPT and 1,3-BDYT interact with SWNT via noncovalent and covalent bindings, respectively. We have also found that 1,3-BDYT tends to be more strongly bound to the metallic SWNT of the smaller diameter. However, 2,4,6-TPPT tends to interact with CNTs via π - π interaction with very small binding energies, regardless of chiralities and diameters.

Keywords: carbon nanotube (CNT), electrophilic molecule, electronic structure

1 INTRODUCTION

Since the first finding on carbon nanotubes (CNTs) [1], there have been extensive investigations on the applications of CNTs. CNTs are fascinating because of their diversity of electronic structure, from metal to semiconductor, depending on their chirality. However, this diversity becomes a major disadvantage in applications of CNTs for real electronic devices. There have been many attempts to separate metallic nanotubes from semiconducting ones, including electrophoresis[2], DNA wrapping[3], electrical breakdown of metallic nanotubes [4], and chemical treatment with various molecules[5-8]. Among them, chemical treatment seems very attractive for a large-scale electronic device fabrication. It was reported that the diazonium compound and nitronium ions selectively attack metallic nanotubes resulting in sorting out semiconducting nanotubes only[5-7]. Recently, our group also reported that some electrophilic molecules can play a similar role to metallic nanotubes to change their electronic structures from the investigations on the electrical transport properties of single-walled CNT field effect transistor reacted with several electrophilic molecules [8]. However, no rigorous explanation has not been suggested for these electrophilic molecules how to affect on the electronic structure of the carbon nanotubes. A few theoretical

approaches have been reported to explain how nitronium ion and diazonium compounds to affect the electronic structures of the carbon nanotubes [9,10]. They suggested that those molecules selectively attack the sidewall of the metallic nanotubes due to the abundant presence of the electron density at the Fermi level. Another theoretical study reported that some large nearly neutral aromatic molecules and some small charge transfer aromatic molecules interact more strongly metallic nanotubes than the semiconducting ones [11].

In the present study, we investigated the interaction of the electrophilic molecules, specifically 1,3-benzodithiolylium tetrafluoroborate (1,3-BDYT) and 2,4,6-triphenylpyrylium tetrafluoroborate (2,4,6-TPPT), with both metallic and semiconducting CNTs in various diameters.

2 COMPUTATIONAL DETAILS

First-principles calculations were performed for the models of 2 electrophilic molecules, 1,3-BDYT and 2,4,6-TPPT on the CNTs of various chiralities. 1,3-BDYT and 2,4,6-TPPT molecules are shown in Fig. 1. The density-functional theory (DFT) was employed using Vienna Ab initio Simulation Package (VASP)[12], and some calculations were done with Dmol³[13]. Generalized gradient approximation (GGA) was adopted for the exchange and correlation with Vanderbilt ultrasoft pseudopotentials. The plan-wave basis sets were used with the energy cutoff as 396 eV. Only Γ -point in k-space is considered for the calculations here.

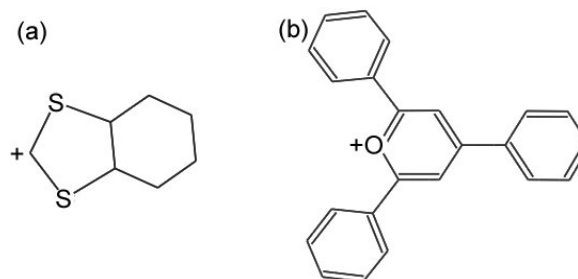


Fig. 1 Electrophilic molecules we considered. (a) 1,3-benzodithiolylium tetrafluoroborate (1,3-BDYT), (b) 2,4,6-triphenylpyrylium tetrafluoroborate (2,4,6-TPPT)

For the small-radius nanotube models, armchair (5, 5) metallic CNT and zigzag (10, 0) semiconducting CNT were chosen, while (10, 10) metallic tube and (17, 0) semiconducting tube were chosen for the large-radius cases. Periodic supercells were taken as containing 3 unitcells for semiconducting tubes and 6 unit cells for the metallic tubes. The sizes of the supercells for the calculations are $24 \times 24 \times 12.68 \text{ \AA}^3$ and $24 \times 24 \times 14.64 \text{ \AA}^3$, for semiconducting tubes and metallic tubes, respectively. Within these supercells, the electrophilic molecule was attached to the sidewall of CNTs, one by one, and the geometric structures were fully relaxed. The atomic relaxation is terminated if the each component of the Hellmann-Feynman force on each atom is reduced to within 0.02 eV/\AA . After structural relaxation of each molecule on the CNT, the binding energy was calculated as the following equation, $E_{\text{bind}} = E_{\text{tot}}(\text{CNT} + \text{mol}) - E_{\text{tot}}(\text{CNT}) - E_{\text{tot}}(\text{mol})$, where E_{tot} is the total energy of a given system

3 RESULTS AND DISCUSSTIONS

3.1 1,3-BDYT on various CNTs

We first studied the single 1,3-BDYT molecule on the side wall of CNT. We have selected the most stable geometry of 1,3-BDYT on metallic or semiconducting CNT, in aqueous solution model. For experimental chemical functionalization, CNTs are immersed into the solution of given electrophilic molecules [8]. In the solution, 1,3-BDYT is dissolved into $(\text{C}_7\text{H}_5\text{S}_2)^+$ and $(\text{BF}_4)^-$ ions. We can suppose that firstly $(\text{C}_7\text{H}_5\text{S}_2)^+$ ion attacks C' atoms of the sidewall of CNT, then the C atom between S atoms of $(\text{C}_7\text{H}_5\text{S}_2)^+$ is covalently bonded to C' atom of the CNT. After C-C' bonding between the electrophilic ion and the CNT, another C1 atom of CNT, which is neighboring to C-

C' bond, becomes active. It is because that the original C1-C' bond becomes weak after C-C' bonding. One can imagine that H^+ ions, which usually exist in aqueous solution, easily attack the active C1 atom, then the H^+ -C1 bond can be formed. From several model calculations of the possible pathways of C-C' bonding, that will be published elsewhere, we have obtained the most stable structure of the covalent bonding between $(\text{C}_7\text{H}_5\text{S}_2)^+$ and CNT with additional H^+ ion adsorption, as shown in Fig. 2-(a)

After adsorption structures were fully relaxed for 4 different CNTs, such as (5,5), (10,0), (17,0) and (10,10), we have calculated binding energies of 1,3-BDYT for each case. The calculated binding energies are plotted with respect to the diameter in Fig. 3. The solid line connects binding energies of 1,3-BDYT on metallic CNTs, whereas the dashed line connects the binding energies on semiconducting CNTs. As shown in Fig. 3, 1,3-BDYT is more strongly bound to the metallic nanotube than the semiconducting nanotube for the smaller diameter.

On the contrary to that, for the larger diameter, such as (10,10) or (17,0) CNT, the binding energies are almost the same for both metallic and semiconducting ones. It infers that 1,3-BDYT is not preferentially bound to the metallic nanotubes anymore for larger diameters, more than 13 \AA . Our previous experiments reported that the yield of selective suppression of metallic nanotubes seems to depend on the diameters of the nanotubes. The best efficiency of selective suppression lies around $10 \sim 20 \text{ \AA}$ [8]. Our calculation results can explain the observed diameter-dependency of selective suppression of metallic nanotubes. The strong adsorption of 1,3-BDYT on metallic CNT can result in changing electronic structure of the metallic nanotubes.

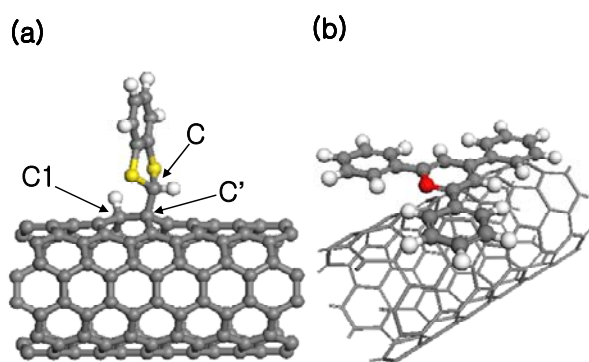


Fig. 2 The optimized structures after full relaxation of (a) 1,3-BDYT with additional H^+ ion, and (b) 2,4,6-TPPT, on (5,5) CNT. Grey balls and sticks are carbons. White ball, yellow ball and red ball represent hydrogen, sulfur and oxygen respectively

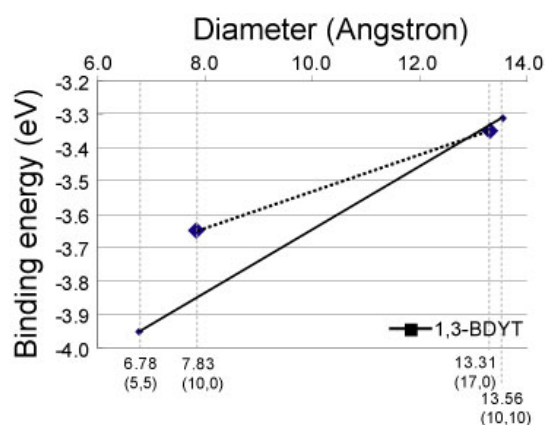


Fig. 3 Binding energies of 1,3-BDYT on CNT are plotted with respect to the diameters and chiralities of CNTs.

3.2 2,4,6-TPPT on various CNTs

Another molecule we have calculated is 2,4,6-TPPT. It consists of 4 aromatic rings, as shown in Fig. 1-(b). 2,4,6-TPPT is dissolved into $(C_{23}H_{17}O)^+$ and $(BF_4)^-$ ions in the solution. We set up the adsorption models of 2,4,6-TPPT on (5,5) and (10,0) nanotubes.

Unlike 1,3-BDYT, 2,4,6-TPPT is expected to be attached to the sidewall of CNT via noncovalent π interaction, because of its planar structure. Moreover, it doesn't need to consider additional H^+ ion adsorption for 2,4,6-TPPT solution, because noncovalent π interaction does not seem to induce any active C site of CNT.

The optimized stable structure of adsorption of 2,4,6-TPPT on CNT is shown in Fig. 2-(b). After adsorption structures were fully relaxed, the binding energies were calculated as -70 meV and -60 meV, for metallic (5,5) nanotube and semiconducting (10,0) nanotube, respectively. There is no difference between metallic and semiconducting nanotubes in the binding energies of 2,4,6-TPPT. However, the experimental effect in selective suppression of metallic nanotubes using 2,4,6-TPPT is very similar to that of 1,3-BDYT [8]. For the case of 2,4,6-TPPT, we need another explanation rather than binding energy difference to explain the experimental results. Recently, Lu et al.[11] suggested that effective contact area and atomistic correlation between aromatic molecules and CNT can lead chiral selectivity. Atomistic correlation between aromatic rings of 2,4,6-TPPT and the hexagonal rings of CNT should be investigated more rigorously to explain chiral selectivity of 2,4,6-TPPT.

4 RAMAN SPECTRA ANALYSIS

In order to investigate the effect of 1,3-BDYT and 2,4,6-TPPT on the CNTs, we had previously performed a Raman spectrum analysis [8]. Fig. 5 shows the Raman spectra of the SWNT-FET device, after reaction with 1,3-BDYT and 2,4,6-TPPT solutions, respectively. The Raman spectra show two peaks, G band and D band, for 1,3-BDYT treatment, while only G band for 2,4,6-TPPT treatment. It is known that the G band near 1600 cm^{-1} is a characteristic peak of pristine CNTs, while the D band near 1350 cm^{-1} is a defect peak. In order to explain this difference between 1,3-BDYT and 2,4,6-TPPT, we have examined the structure of adsorption geometry and have calculated charge density of the given system. Figure 6 shows the charge density plot of the final geometry containing (a) 2,4,6-TPPT and (b) 1,3-BDYT on (5,5) CNT, respectively. 1,3-BDYT forms chemical bonding with C atom of CNT, whereas 2,4,6-TPPT lies above the sidewall of CNT at a distance of 3.43 \AA , where is van der Waals interaction region. 2,4,6-TPPT interacts with CNT non-covalently via π - π interaction. Thus there is no significant structural distortion of CNT. It explains the only G band appears in the Raman spectra of 2,4,6-TPPT treatment. On the contrary, 1,3-BDYT is

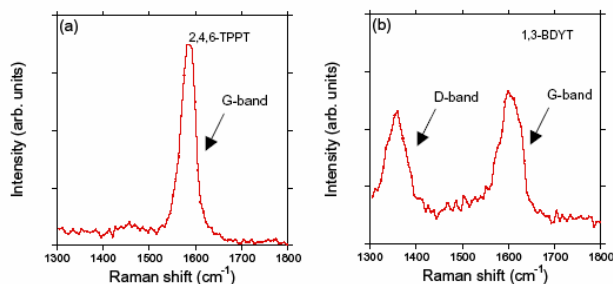


Fig.4 D, G band of Raman spectra of the SWNT-FET device after reaction with (a) 2,4,6-TPPT and (b) 1,3-BDYT treatment.

covalently bound to CNT and forms sp^3 -like bond, which is the origin of D band in Fig. 6-(b).

5 CONCLUSIONS

In this study, we present systematic theoretical studies on the interactions between the CNTs and the electrophilic molecules, such as 2,4,6-TPPT and 1,3-BDYT. We have used the first principle method based on density functional theory. Firstly, we have calculated the binding energies of these two electrophilic molecules on the several CNTs including both metallic and semiconducting ones with different diameters, such as (5,5), (10,0), (17,0) and (10,10). We have found that 1,3-BDYT tends to be more strongly bound to the metallic SWNT in the smaller diameter less than 13 \AA . However, 2,4,6-TPPT tends to interact with CNTs via π - π interaction with very small binding energies about 60-70 meV, regardless of chiralities and diameters. We have also shown that 2,4,6-TPPT and 1,3-BDYT interact with CNT via noncovalent and covalent bindings, respectively. It can explain the observed Raman spectra of CNTs with 2,4,6-TPPT and 1,3-BDYT treatment. Additional D band observed in 1,3-BDYT treatment is well explained with sp^3 bond formation between 1,3-BDYT and CNT. From these calculations, we can conclude that electrophilic molecule tends to more strongly bind to the

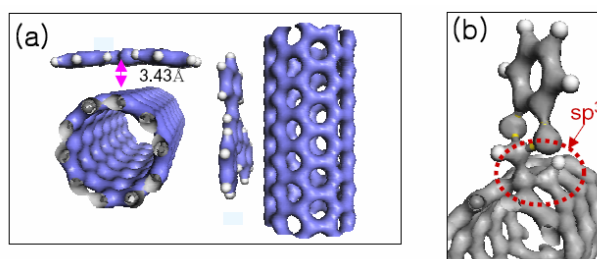


Fig.5 Optimized structures of SWNT and (a) 2,4,6-TPPT, and (b) 1,3-BDYT. The calculated total electron densities are also shown in blue and gray for (a) 2,4,6-TPPT and (b) 1,3-BDYT, respectively

metallic CNT than to the semiconducting CNT, at the small diameter region, when it forms covalent bonding. Its strong binding leads to change in electronic structures of metallic nanotube via forming *sp*³ configuration. It seems to result in selective suppression of metallic nanotubes.

ACKNOWLEDGEMENTS

This work was supported by the Korea Research Council for Industrial Science & Technology.

REFERENCES

- [1] Ijima, S. *Nature*, **1991**, 354, 56.
- [2] Krupke, R.; Hennrich, F.; von Lohneysen, H.; Kappes, M. M. *Science*, **2003**, 301, 344.
- [3] Zeng, M.; Jagota, A.; Semke, E. D.; Diner, B. A.; Mclean, R. S.; Rustig, S. R.; Richardson, R. E.; Tassi, N. G. *Nat. Mater.* **2003**, 2, 338.
- [4] Collins, P. G.; Arnold, M. S.; Avouris, P. *Science* **2001**, 292, 706.
- [5] Strano, M. S.; Dyke, C. A.; Usrey, M. L.; Baron, P. W.; Allen, M. J.; Shan, H.; Kittrell, C.; Hauge, R. H.; Tour, J. M.; Smalley, R. E. *Science* **2003**, 301, 1519.
- [6] Maeda, Y. et al. *J. Am. Chem. Soc.* **2005**, 127, 10287.
- [7] An, K. H.; Park, J. S.; Yang, C.-M.; Jeong, S. Y.; Lim, S. J.; Kang, C.; Son, J.-H.; Jeong, M. S.; Lee, Y. H. *J. Am. Chem. Soc.* **2005**, 127, 5196.
- [8] So, H.-M.; Kim, B.-K.; Park, D.-W.; Kim, B. S.; Kim, J.-J.; Kong K.-j.; Chang, H.; Lee, J.-O. *J. Am. Chem. Soc.*, **2007**, 129, 4866.
- [9] An, K. H.; Yang, C.-M.; Seo, K.; Park, K. A.; Lee, Y. H. *Current Applied Physics*, **2006**, 6S1, e99.; Yang, C.-M.; Park, J. S.; An, K. H.; Seong, C. L.; Seo, K.; Kim, B.; Park, K. A.; Han, S.; Park, C. Y.; Lee, Y. H. *J. Phys. Chem. B.* **2005**, 109, 19242.
- [10] Du, A.J.; Smith, S. C. *Molecular Simulation*, **2006**, 32, 1212.
- [11] Lu, J.; Nagase, S.; Zhang, X.; Wang, D.; Ni, M.; Maeda, Y.; Wakahara, T.; Nakahodo, T.; Tsuchiya, T.; Akasaka, T.; Gao, Z.; Yu, D.; Ye, H.; Mei, W. N.; Zhou, Y. *J. Am. Chem. Soc.* **2006**, 128, 5114.
- [12] G. Kresse and J. Hafner, *Phys. Rev. B*, **1993**, 47, 558.; *ibid.*, **1994**, 49, 14251.; G. Kresse and J. Furthmueller, *ibid.*, **1996**, 54, 11169.
- [13] DMol³ is a registered software product of Accelrys, Inc. Delley, B. *J. Chem. Phys.* **1990**, 92, 508.